M'zali, N.; Henneron, T.; Benabou, A.; Martin, F.; Belahcen, A.

Finite Element Analysis of the Magneto-mechanical Coupling Due to Punching Process in Electrical Steel Sheet

Document Version
Peer-reviewed accepted author manuscript, also known as Final accepted manuscript or Post-print

Finite Element Analysis of the Magneto-mechanical Coupling Due to Punching Process in Electrical Steel Sheet

N. M'zali[1,2], T. Henneron[1], A. Benabou[1], F. Martin[2], A. Belahcen[2], *Senior Member*, *IEEE*

[1]Univ. Lille, Arts et Metiers Institute of Technology, Centrale Lille, Junia, ULR 2697 - L2EP, F-59000 Lille, France
[2]Department of Electrical Engineering and Automation, Aalto University, Aalto FI-00076, Finland

In this paper, a finite element (FE) modeling of the punching effect on the magnetic properties of electrical steel sheet is carried out. For that, the modified anhysteretic Sablik model is applied together with the plastic strain distribution obtained from a punching process simulation performed using the software ABAQUS. First, a synchronous electrical machine is simulated including the effect of the punching process, it shows the degradation of the magnetic flux density at the lamination edges and an increase of the iron losses. Then, results obtained from the magneto-mechanical simulation are investigated in terms of the method used to implement the plastic strain distribution in the FE computation. Two examples have been investigated: a square steel sheet and a tooth of an electrical machine.

Index Terms — **Magneto-mechanical modeling, Plastic strain distribution, Punching effect, Finite element method.**

I. INTRODUCTION

The stator core of an electrical machine undergoes different shaping and assembly processes, which lead to the accumulation of mechanical deformation and the degradation of magnetic properties. It is shown that the iron losses increase and the magnetic permeability decreases [1]. Among possible manufacturing processes, mechanical punching is the most used for large series production of electrical machines. It induces plastic strain which is concentrated near the punching edges thus delimiting a "deformation affected zone" (DAZ) [2].

To anticipate the effect of these degradations on the magnetic performances, the effect of punching must be integrated in the design process of electrical machines. Usually, studies consider the effect on the magnetic behavior via empirical approaches [3]. In the present work, we consider the implementation of a magneto-mechanical model that directly accounts for the plastic strain [4]. Although the plastic strain distribution can be approximated through micro-hardness measurements [5], we chose to perform a realistic mechanical simulation of the punching process based on [6]. The full spatial distribution of the plastic strain is often approximated by a "degradation profile" which is an exponential function of the distance from the punching edge [7].

With respect to this background, we propose to extend our previous work [8], which details a punching process simulation, with a simplification toward a 2D implementation for modelling the performance of an electrical machine. This paper investigates first the effect of such assumption, by considering the degradation profile on the iron loss of a synchronous electrical machine. Then, we will more closely consider the method used to account for the plastic strain at the punching edge, especially by comparing the magnetic behavior of punched specimen with elementary geometries when the full plastic strain field is considered and when the degradation profile is used. Two examples have been considered: the initial reference steel sheet sample and a tooth of an electrical machine.

II. MAGNETO-MECHANICAL MODELING

The anhysteretic Sablik model, studied in a previous work [8], is considered to model the magneto-mechanical coupling induced by the punching process. A brief reminder of the main aspects is given.

A. Magneto-plastic model

The Sablik model is based on the thermodynamic equilibrium, where the anhysteretic magnetization M_{an} is expressed with the Langevin function [9].

$$M_{an} = M_s \left(\coth\left(\frac{H_e}{a}\right) - \frac{a}{H_e} \right) \tag{1}$$

$$H_e = H + \alpha M_{an} + H_\sigma \tag{2}$$

where M_s, M_{an}, H, and H_e are the saturation magnetization, anhysteretic magnetization, applied magnetic field, and the effective magnetic field, respectively. α is a parameter representing the inter-domain magnetic coupling and a is the anhysteretic scaling factor. H_σ is the component of the effective field due to the mechanical stress.

$$H_\sigma = \frac{3}{2} \frac{\sigma}{\mu_0} \left(\frac{\partial \lambda}{\partial M_{an}} \right)_T \tag{3}$$

$$\lambda = \left(a_1 M_{an}^2 \right) \left(C + \tanh\left(\frac{\sigma - \sigma_0}{\tau}\right) \right) \tag{4}$$

where μ_0 and σ are the permeability of the vacuum and the mechanical stress, respectively. λ is the magnetostriction function, which depends on the magnetization and the stress, with a_1, C, τ and σ_0 its parameters. The effect of the plastic deformation is considered in the model by writing the anhysteretic form factor a as a function of the dislocation density ξ_d [4] such that,

$$a = \left(G_1 + \frac{G_2}{d} \right) a_0 \xi_d^{\frac{1}{2}} \tag{5}$$

with G_1 and G_2 two constants related to the grain size d, and a_0 is the anhysteretic form factor prior to plastic deformation. The dislocation density ξ_d is expressed as:

$$\xi_d = \left(\left(\frac{\sigma_F}{0.76Gb} \right) + \xi_{d0}^{1/2} \right)^2 \qquad (6)$$

$$G = \frac{Y}{2(1+\upsilon)} \qquad (7)$$

where ξ_{d0} is the initial dislocation density prior to the plastic deformation, G is the specimen shear modulus as given by (7), b is the appropriate Burger vector magnitude for the specimen dislocations, υ is the Poisson ratio, Y is the Young modulus. σ_F represents the hardening stress that is related to the plastic strain ε by the Ludwik law $\sigma_F(\varepsilon) = k_F \varepsilon^{n_F}$, k_F is the hardening coefficient and n_F the Ludwik exponent.

B. Model identification

The identification of the Sablik model parameters is carried out by fitting the model with measured magnetization curves for different elastic stress and plastic strain levels following three distinct steps.
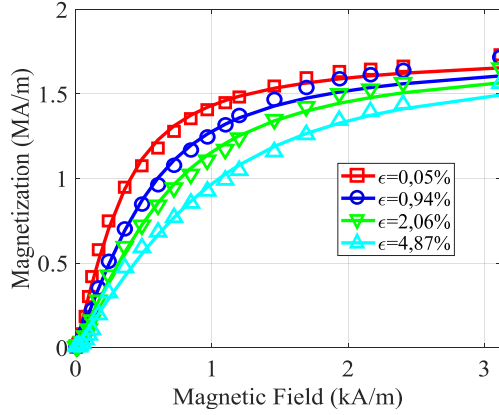

Fig. 1. Measured (dashed line) and modeled (solid line) magnetization curves for different values of plastic strain. Y=174 GPa, υ=0.3, b=10×10^{-10} m, ξ_{d0}=0.55×10^{12}/m^2, d=30×10^{-6} m G_1=10^{-6} m, G_2=1.07×10^{-11} m^2. a_0=120.86 M_s=1.39×10^6 A/m, α=4.10×10^{-5}. a_1-1.69×10^{-18}, C=-0.94, τ = 24.54 MPa σ_0 = 8.29 MPa, n_F=0.43, k_F=701.8 MPa.

First, without considering the stress dependence in (2) ($H_\sigma = 0$), the initial parameters of the model: a, M_s, and α are identified. Second, the elastic stress dependence is considered in (2) ($H_\sigma \neq 0$), and the parameters a_1, C, τ and σ_0 are identified. Finally, the plastic dependency given by (4) is introduced in (1), and the plastic parameters G_1, G_2, ξ_{d0} are identified. The results of this identification are given in Fig. 1 with the corresponding parameters in the caption.

III. DEGRADATION PROFILE APPROACH

In this section the effect of punching process on the stator of a buried permanent magnet synchronous machine is simulated.

A. Plastic strain distribution and degradation profile

To estimate the distribution of the plastic strain due to the punching process, a mechanical simulation has been carried out using the ABAQUS software for a steel sheet sample with a thickness t = 0.5 mm. The considered simulation approach is based on the equivalent plastic strain and the plan [6]. The detail of the simulation parameter is given in [8].

Figure 2-a gives the distribution of the plastic strain in the DAZ. A plastic strain profile can be derived by averaging the equivalent plastic strain along the cutting direction (y axis in Fig. 2b).
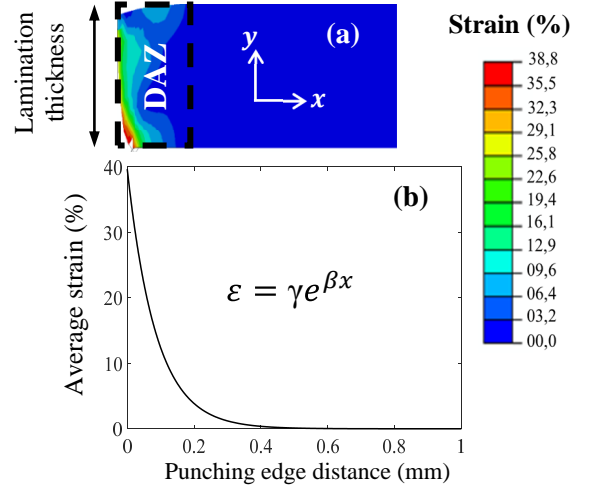

Fig. 2. Distribution of the plastic strain in the DAZ ($\gamma = 39.66$, $\beta = -11.64$)

B. Synchronous machine simulation

The mesh and the description of the 5-phase synchronous machine are given in Figure 3. Due to the lack of magnetic symmetry, the whole cross section is modeled. A no-load simulation, at speed 750 rpm (corresponding to 87.5Hz stator frequency), has been carried out using the magnetic vector potential formulation. The punching effect is considered in the numerical model by using the calculated degradation profile (Fig.2-b). The punching effect is considered on the whole perimeter of the stator yoke, including the teeth and slot edges. For each integration point of each element of the stator mesh, the normal distance from the cutting edge is calculated in order to determine the corresponding plastic strain that is used in the Sablik model.
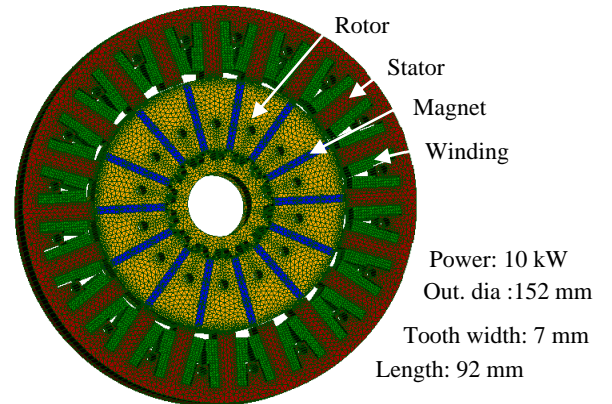

Fig. 3. Description of the simulated synchronous machine

In Fig.4-a, the resulting magnetic flux density is given, and Fig.4-b shows the difference in terms of magnetic flux density between simulations with and without consideration of the punching effect. The decrease of magnetic flux density at the lamination edge can reach about 0.4 T, which is significant.

In addition to the magnetic behavior, the degradation has also an impact on the hysteresis losses. Therefore, to estimate the iron losses (P) in the electrical machine, the Jordan model given in (8) is applied as a first approach.

$$P = k_\text{h}(\varepsilon)\, f B^{\alpha(\varepsilon)} \ + \ k_\text{cl} f^{\,2} B^2 \tag{8}$$

As mainly static losses are affected by the cutting, the hysteresis loss parameters k_h and α are considered depending on the plastic strain. The parameter k_cl is related to the classical eddy current losses (supposed to be unaffected by the cutting) and f is the frequency.
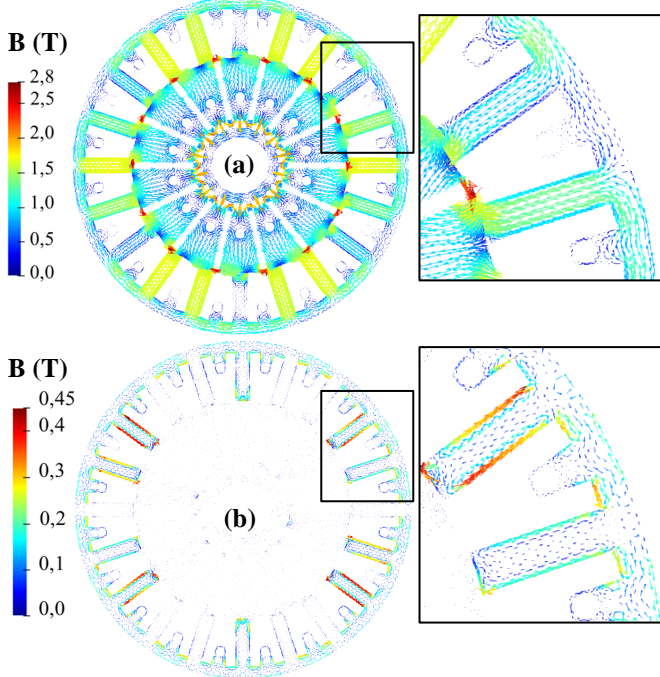

Fig. 4. (a) Magnetic flux density distribution considering punching effect (b) Difference between cases with and without the punching effect.

The evolutions of static parameters were identified using loss measurement under different plastic strains (Fig.5).
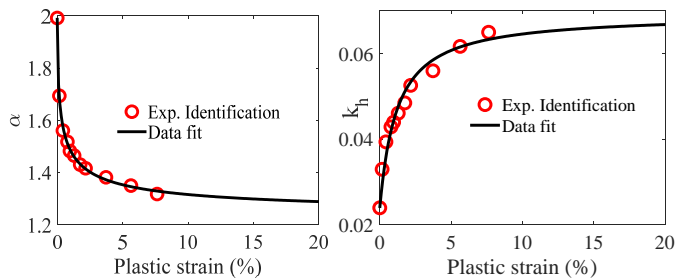

Fig. 5. Evolution of the loss model parameters with respect to the strain

Table I gives the core losses in the stator yoke calculated with and without considering the punching process effect, it is shown that it increased by about 38%.

TABLE I
SIMULATED CORE LOSS WITH AND WITHOUT PUNCHING EFFECT

Core loss without punching	Core loss with punching
25.55 W	35.40 W

IV. COMPARISON OF DEGRADATION PROFILE AND FULL STRAIN DISTRIBUTION

The identification of the degradation profile with the average equivalent plastic strain (Fig.2-b) is now compared with a 2D extruded mechanical simulation based on the full strain distribution along the sheet thickness. The analysis is conducted by comparing the magnetic energy for two examples: a steel sheet sample and a tooth of an electrical machine.

A. FE analysis – steel sheet

The 2D model of the punched steel sheet is extruded to form a 3D model in order to be in the same condition as the electrical machine tooth. From this result a steel sheet punched on two sides is generated by mirroring. A magnetostatic problem, using the magnetic vector potential formulation, with an imposed magnetic flux along the z-axis (parallel to the cutting edges) is solved for the sample geometry [10].

Figure 6 presents the magnetic flux density in the steel sheet punched on two sides obtained when the strain distribution is considered and when a degradation profile is used. It can be noticed that the volume and morphology of the impacted areas are different. To assess this difference from the modelling point of view, the magnetic energy is analyzed.
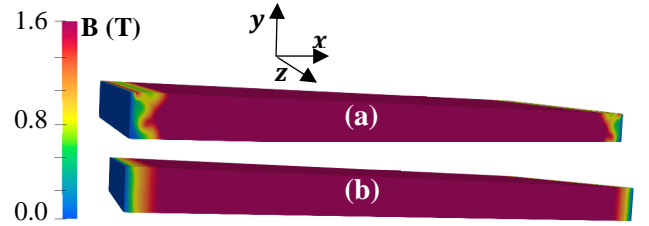

Fig. 6. Magnetic flux density map in the steel sheet considering (a) the full plastic strain distribution (b) the averaged strain profile. Sample dimensions: length = 6 mm, width = 3 mm, thickness t = 0.5 mm.
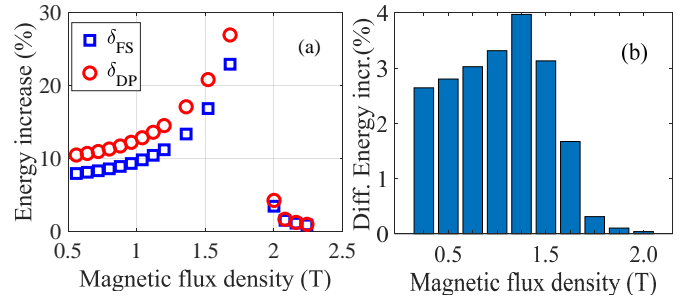

Fig. 7. (a) Evolution of δ_FS and δ_DP for different imposed magnetic flux (b) difference in increase of magnetic energy $\delta_\text{DP} - \delta_\text{FS}$.

Fig. 7 shows the relative increase δ in the total magnetic energy for different imposed magnetic flux magnitudes, such that $\delta = (\text{E}_\text{d} - \text{E}_0)/\text{E}_0$, where E_d and E_0 represent the magnetic energy with and without considering the punching effect, respectively. Quantities δ_FS and δ_DP refer to the increase of the magnetic energy when the full strain distribution is considered, and when the degradation profile is used, respectively. As expected, because the magnetic flux is imposed, the magnetic energy increases when the material properties are degraded. In Fig.7-a, δ_FS and δ_DP are presented with respect to the average

magnetic flux density (imposed magnetic flux divided by the sample cross section). Although they show the same behavior, δ_{DP} has higher amplitude. The difference $\delta_{DP} - \delta_{FS}$ given in Fig. 7-b is explained by the plastic strain effect that is relatively lower for magnetic flux densities located in the linear zone of BH curves (Fig.1), then maximum at intermediate flux densities and negligible in the saturation zone. Thus, δ_{FS} and δ_{DP} as well as their difference are relatively small for low magnetic flux densities; they reach a maximum at about 1.3 T and then become minor at saturation.

Figure 8 gives the evolution of δ_{FS} and δ_{DP} for different widths of the steel sheet punched on two sides, the average magnetic flux density is kept fixed at around 1.4 T. It is shown that for small width sheet where the DAZ occupies a significant proportion of the total sheet volume, δ_{DP} is significantly higher than δ_{FS}. As expected, the difference between both methods becomes minor for large width sheets.
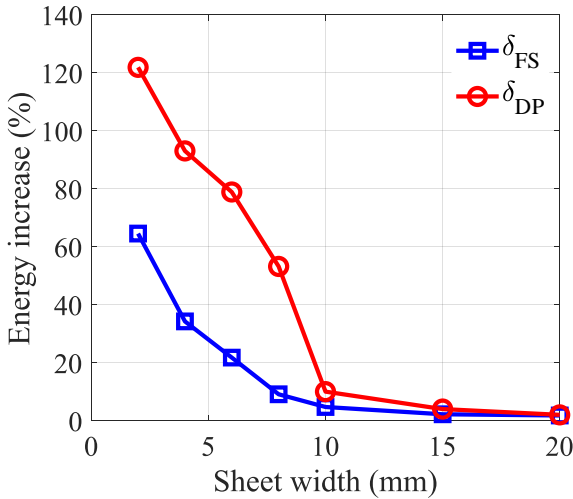

Fig. 8. Evolution of the magnetic energy increase due to the punching effect for different sheet widths punched on two sides.

B. FE analysis – tooth of an electrical machine

In this section, we consider a typical tooth of small electrical machine where the punching is expected to have a significant impact. The tooth dimensions correspond to a real industrial machine where the stator yoke thickness is d_y = 5 mm and the average tooth body width is τ =2 mm. To define the plastic strain distribution near the tooth edges, a 3D punching process simulation is performed. The magnetostatic problem is considered by imposing the magnetic flux to enter through the tip of the tooth and exit at both lateral sides of the yoke.

Figure 9 gives the magnetic flux density distribution considering the full plastic strain distribution and the degradation profile. The difference between both distributions is not obvious to distinguish from one another. However, the analysis in terms of magnetic energy shows a great disparity with δ_{FS} = 87 % and δ_{DP} = 180 %. This result confirms the behavior investigated in the steel sheet and shows that the way the degradation profile is determined should be carefully considered to have a realistic representation of the global magnetic behavior.
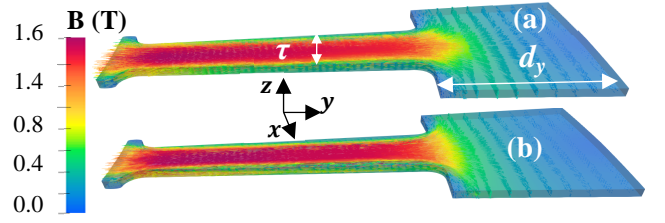

Fig. 9. Magnetic flux density in the tooth considering (a) the full plastic strain distribution (b) the degradation profile.

V. Conclusion

Using the magneto-mechanical Sablik model and strain-dependent loss parameters, the impact of the punching process on the magnetic properties has been investigated. Although the preliminary analysis of the synchronous machine was performed with the degradation profile for achieving some realistic computational time, it shows a significant increase of iron loss, about 38 %. It has also been shown that the degradation profile defined by the average value of the strain at each position from the edge does not reflect the real plastic strain distribution in the steel sheet depth. Indeed, depending on the magnetic flux density amplitude and the dimensions of the simulated problem, the magneto-mechanical behavior varies substantially. However, the use of the full plastic strain to simulate an electrical machine would lead to a significant computation time as it requires a fine mesh along the punching edges. In that context, a degradation profile is more practical, but improvements are still needed in order to be closer to the reference behavior (full plastic strain distribution). For example, one can consider the adjustment of the degradation profile based on the results obtained with the reference case.

References

[1] N. Leuning, *et al*, "Effect of elastic and plastic tensile mechanical loading on the magnetic properties of NGO electrical steel," *J. Magn. Magn. Mater.*, vol. 417, pp. 42–48, 2016.

[2] Z. Wang *et al.*, "Influence of Grain Size and Blanking Clearance on Magnetic Properties Deterioration of Non-Oriented Electrical Steel," *IEEE Trans. on Magn*, vol. 54, no. 5, pp. 1–7, May 2018.

[3] R. Sundaria *et al*, "Effect of Laser Cutting on Core Losses in Electrical Machines Measurements and Modeling," *IEEE Transactions on Industrial Electronics*, vol. 67, no. 9, pp. 7354–7363, Sep. 2020.

[4] M. J. Sablik *et al.*, "Modeling plastic deformation effects in steel on hysteresis loops with the same maximum flux density," *IEEE Trans. on Magn.*, vol. 40, no. 5, pp. 3219–3226, Sep. 2004.

[5] H. A. Weiss *et al.*, "Influence of shear cutting parameters on the electromagnetic properties of non-oriented electrical steel sheets," *J. Magn. Magn. Mater*, vol. 421, pp. 250–259, Jan. 2017.

[6] H. Marouani, *et al*, "Rate-dependent constitutive model for sheet metal blanking investigation," *Mater. Sci. Eng., A*, vol. 487, no. 1–2, pp. 162–170, Jul. 2008.

[7] M. Bali and A. Muetze, "Modeling the Effect of Cutting on the Magnetic Properties of Electrical Steel Sheets," *IEEE Trans. Ind. Elec.*, vol. 64, no. 3, pp. 2547–2556, Mar. 2017.

[8] N. M'zali, *et al.,* "Finite-Element Modeling of Magnetic Properties Degradation Due to Plastic Deformation," *IEEE Trans. on Magn.*, vol. 56, no. 2, pp. 1–4, Feb. 2020.

[9] D. C. Jiles and D. L. Atherton, "Theory of ferromagnetic hysteresis," *J. Magn. Magn. Mater.*, vol. 61, no. 1, pp. 48–60, Sep. 1986.

[10] T. Henneron, *et al*, "Discrete finite element characterizations of source fields for volume and boundary constraints in electromagnetic problems," *J. Comput. Appl.*, vol. 215, no. 2, pp. 438–447, Jun. 2008.